

Picosecond surface acoustic waves using a suboptical wavelength absorption grating

D. H. Hurley and K. L. Telschow

Idaho National Engineering and Environmental Laboratory, Idaho Falls, Idaho 83415

(Received 23 May 2002; published 1 October 2002)

We have demonstrated laser generation and detection of Rayleigh surface acoustic waves (SAW's) with acoustic wavelengths that are smaller than the optical wavelength of both the excitation and the detection beams. SAW generation was achieved using electron beam lithography to modulate the surface reflectivity and hence the lateral thermal gradients on a suboptical wavelength scale. The generation and detection characteristics of two material systems were investigated (aluminum absorption gratings on Si and GaAs substrates). The polarization sensitive absorption characteristics of the suboptical wavelength lithographic grating were exploited in order to explore various acoustic generation and detection schemes.

DOI: 10.1103/PhysRevB.66.153301

PACS number(s): 63.20.-e, 43.38.+n, 63.22.+m, 68.35.-p

Laser picosecond acoustics is receiving growing attention because of its ability to characterize ultrafast carrier dynamics in material systems with nanometer length scales.^{1,2,3} Picosecond acoustics typically involves laser generation and detection of longitudinal acoustic waves with wavelengths that are smaller than the optical wavelength of the excitation beam.^{4,5} Acoustic generation entails irradiating a sample with a short, very intense laser pulse (pump beam) and subsequent conversion of the absorbed laser energy into acoustic phonons via a variety of mechanisms⁶ (thermoelastic, concentration deformation, piezoelectric). Laser detection (probe beam) of the acoustic pulse is accomplished by either monitoring strain induced changes in the reflectivity or using interferometric techniques to resolve real and imaginary modulations of the refractive index as well as phase changes caused by surface displacement.⁷

There remains much scope for future investigation in this field. For example, generation of SAW's with nanometer size wavelengths would provide a new acoustic mode for characterizing physical processes. The transverse and longitudinal character of SAW's could be exploited to access a greater number of material properties of nanostructures. However, to date, laser generation of SAW's with acoustic wavelengths smaller than the optical wavelength of the pump and/or probe beam has not been reported.

For the case of optoacoustic generation using subpicosecond laser pulses, the spatial extent of the acoustic disturbance is related to the acoustic transit time across a particular dimension of the effective absorption volume.⁸ The effective absorption volume is represented as $\zeta_z(\delta, \kappa, g)\zeta_r^2(x, y)$, Fig. 1, where ζ_z is the vertical extent of the absorption volume, δ is the optical skin depth, κ is the thermal conductivity, g is the electron-phonon coupling constant, and ζ_r is the lateral extent of the absorption volume. For bulk longitudinal wave generation, ζ_z is the pertinent length scale and for SAW generation, ζ_r is the pertinent length scale. Typical values for ζ_z for metallic films are in the 10–100 nm range⁸ and using conventional focusing techniques, typical values for ζ_r are proportional to the diffraction limited spot size $q_0 \sim 1 \mu\text{m}$. Thus, production of picosecond SAW's can be achieved by spatially modulating the refractive index at the sample surface on a length scale smaller than q_0 . This can be accomplished by using electron beam lithography to deposit a pe-

riodic series of metallic bars (absorption grating) on semitransparent substrates. For SAW generation in this fashion, the absorbed laser energy is converted into a SAW having the same spatial period as the grating and a propagation direction that is perpendicular to the bar/grating axis.

Similar to the generation process, the detection bandwidth of SAW's is governed by the acoustic transit time across the absorption volume of the probe beam. Current detection techniques that use diffraction limited spots produce a detection bandwidth in the low GHz range.⁹ However, for the present case, the generation and detection beam spatially overlap. Thus the spatial period of the grating determines both the generation and detection bandwidth.

Previous studies^{10,11} have used pump-probe methods to investigate the acoustic response of a periodic array of metallic bars attached to semitransparent substrates. Lin *et al.*¹⁰ argued that for gold bars on a silica substrate, strong coupling to bulk longitudinal modes greatly inhibited SAW generation efficiency. They attributed the measured signal to acoustic normal modes of the individual bars.

Attenuation of the SAW caused by coupling to bulk modes can be qualitatively understood by considering a thin elastically isotropic grating on an elastically isotropic substrate. The magnitude of the Poynting vector corresponding to bulk wave radiation can be represented by $P_y = A(h^2\rho_m^2)/(p^4)$, where A depends on the density and elastic constants of the substrate, h is the height of the metallic bars, ρ_m is the mass density of the metal, and p is the grating

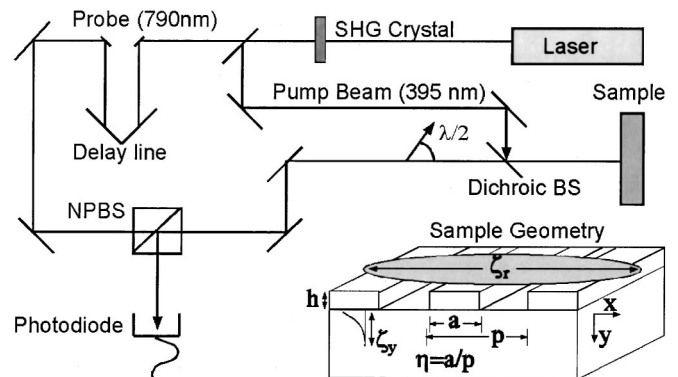


FIG. 1. Experimental setup and sample geometry.

period,^{10,11} Fig. 1. Capitalizing on this relationship between generation efficiency and mass density, Bonello *et al.*¹¹ recently demonstrated laser generation and detection of SAW's by utilizing relatively light aluminum bars¹² on a silicon substrate. They produced 5 GHz SAW's using 750 nm pump light and a bar repeat length of 1 μm .

The present case investigates the unique generation and detection characteristics of a suboptical wavelength absorption grating. Two samples were prepared using electron beam lithography. They consisted of 5 μm long bars periodically deposited on (100) Si and (100) GaAs substrates. For the Si sample, the bar axis coincided with the [001] direction and for the GaAs sample the bar axis coincided with the [011] direction. The Rayleigh velocities, determined from the elastic constants, for the unloaded Si and GaAs samples described above are 4.92 and 2.72 nm/ps, respectively. The bar height h was approximately 50 nm and the periodicity p was 220 nm. The metallization duty cycle η was approximately 50 and 70 % for the Si and GaAs substrates respectively. The experimental setup is shown in Fig. 1. The pump and probe pulse trains are derived from the same femtosecond Ti: sapphire laser (Coherent Mira 900) with ~ 100 fs pulse duration and a 76 MHz repetition rate. The 790 nm output was used for the probe beam while the second harmonic at 395 nm was used for the pump beam. The pump beam was modulated at 1 MHz to facilitate lock-in detection. The pump and probe beams were combined using a dichroic beam splitter to allow both beams to pass through the same $50 \times$ microscope objective producing a 2 μm spot at the sample surface.

The acoustic generation and detection characteristics of the suboptical wavelength absorption grating ($\lambda_{\text{probe}} \sim 4p$)^{13,14} were examined by varying the optical polarization relative to the grating axis of both the pump and probe beams, Fig. 2. Data presented in Figs. 2(b) and 2(c) involve varying the polarization of the probe beam relative to the grating axis while keeping the polarization of the pump beam aligned with the grating axis. Data presented in Fig. 2(d) involve varying the polarization of the pump beam relative to the grating axis while keeping the polarization of the probe beam aligned with the grating axis. The change in reflectivity for a uniform aluminum film deposited at the same time as the grating, and a pristine Si substrate are represented in Fig. 2(a) (i) and (ii), respectively. The sharp change in the two signals near $t=0$ is caused by nonequilibrium heating and rapid cooling (<1 ps) of the electron gas.¹⁵ These changes are followed by a slow decay caused by thermal diffusion. In the case of the aluminum film there is a periodic modulation (~ 62 GHz) caused by reverberation of the acoustic pulse inside the film, which was used to estimate the bar thickness. The thermal response of Si and aluminum are of opposite sign suggesting a method for separating physical processes that occur in the aluminum grating and Si substrate. A comparison between two detection schemes, optical polarization of probe beam parallel (i) and perpendicular (ii) to the grating axis, is presented Fig. 2(b). The sign of the thermal response for the parallel and perpendicular detection schemes is of the same sign as the thermal response of the uniform aluminum film and the Si substrate, respectively. This observation strongly suggests that the absorption grating acts as an

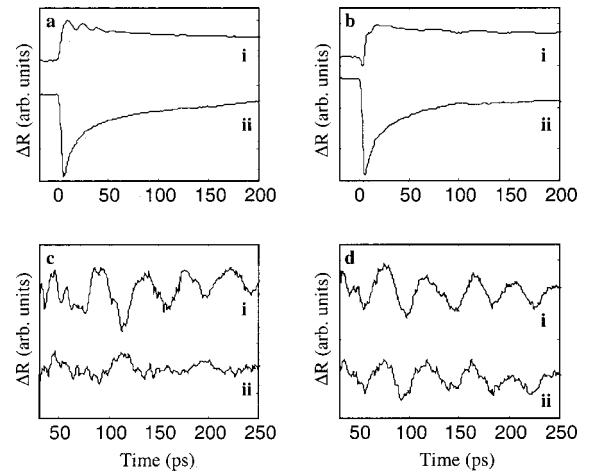


FIG. 2. (a)–(c) Detection characteristics, (d) generation characteristics. (a) Change in reflectivity (ΔR) for a uniform aluminum film (i) and for a pristine Si substrate (ii). (b) ΔR for an aluminum absorption grating, the optical polarization of the probe is parallel (i) and perpendicular (ii) to the bar axis. (c) Corresponds to data presented in (b) with the thermal background removed, the probe polarization is parallel (i) and perpendicular (ii) to the bar axis. (d) ΔR for the aluminum grating, with the thermal background removed, the optical polarization of the pump is parallel (i) and perpendicular (ii) to the bar axis.

optical polarizer for the 790 nm probe light. The data presented in Fig. 2(c) (i) and (ii) correspond to Fig. 2(b) (i) and (ii), respectively, with the thermal background removed. The ratio of the peak Fourier amplitudes ($A_{\parallel}/A_{\perp} = 3.9$) exhibits the enhanced sensitivity of the parallel detection scheme. It is of interest to note that the results obtained using the two detection schemes are out of phase by approximately 180° . A possible explanation for this phase difference can be elucidated by examining the nature of the physical processes contributing to the modulation of the probe beam for the two detection schemes. In the parallel detection scheme, modulation of the probe beam is a result of photoelastic coupling to the strain field in the grating material. In the perpendicular scheme, modulation of the probe beam stems from both photoelastic coupling to the strain field in the substrate material and acoustic modulation of the diffraction characteristics of the grating.

A comparison for the two generation schemes, optical polarization of the pump parallel (i) and perpendicular (ii) to the grating axis, is presented in Fig. 2(d). In this case the ratio of the Fourier amplitudes $A_{\parallel}/A_{\perp} = 1.2$, implies that the absorption characteristics of the aluminum grating are only slightly polarization selective for the 395 nm pump light. The weak polarization selectivity for the 395 nm pump beam as compared to the 790 nm probe beam is in keeping with previous studies involving lithographic wire grid polarizers.^{13,16}

Figure 3 compares the change in reflectivity for the Si and GaAs samples. The center frequency for the Si and GaAs samples is 23 and 13 GHz, respectively. These frequencies correspond closely to the frequency predicted using the Rayleigh velocity of the substrate material and the grating period $f = V_R/p$ (22.4 and 12.4 GHz for Si and GaAs,

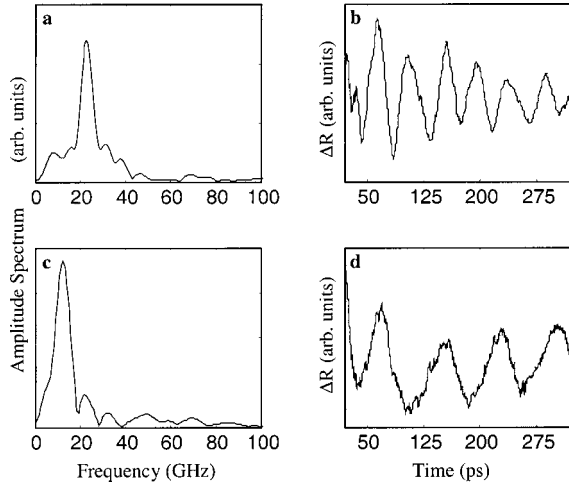


FIG. 3. (a),(c) Magnitude of the Fourier transform of the change in reflectivity for Si and GaAs, respectively. (b),(d) Change in reflectivity for Si and GaAs, respectively.

respectively).¹⁷ The assumption that the Rayleigh velocity across the grating region is the same as that of the pristine substrate has been used in previous studies to prove/disprove the existence of surface acoustic waves. For gold bars on a fused quartz substrate, Lin *et al.*¹⁰ argued against the generation of SAW's since the measured frequency did not change as a function of period according to $f = V_R/p$. Bonello *et al.*,¹¹ for the case of aluminum bars on a silicon substrate with a 1 μm period, varied that metalization ratio as a way of isolating SAW's from normal modes of the individual bars. However, for increasing frequencies and decreasing grating periods, the effect of mechanical loading as a function of both the metalization ratio and grating period can alter the SAW velocity from that of a pristine substrate. For instance, Koskela *et al.*¹⁸ have demonstrated suppression of bulk wave radiation in LiNbO₃ by slowing the leaky-SAW velocity below the slow surface skimming shear wave velocity using heavy mechanical loading provided by a Au grating. For $h/\lambda = 0.025$, a 10% reduction in velocity was demonstrated.

In order to qualitatively explore the influence of mechanical loading on the SAW velocity; consider a perturbation theory first presented by Auld.¹⁹ The theoretical development involves expanding the interface stress (interface between the substrate and bar material) in a Taylor series about the strip height. Retaining only first order terms, the change in phase velocity can be expressed as $\Delta V/V = F_v(h/p)\eta$, where F_v is the first order mechanical scattering coefficient. The method for obtaining F_v is outlined in Refs. 20,21 and only the results for specific cases will be given presently. For the sake of understanding the present study in the context of previous efforts, the predicted velocity perturbations caused by gold bars as well as aluminum bars will be presented. For the GaAs system, (100) plane and [011] propagation direction, $\Delta V/V|_{\text{Al}} = 0.24(h/\lambda)\eta$ and $\Delta V/V|_{\text{Au}} = -5.11(h/\lambda)\eta$. Piezoelectric coupling for this system is small and the effect of piezoelectric shorting on the velocity was neglected. For the Si system, (100) plane and [010] propagation direction, $\Delta V/V|_{\text{Al}} = -1.26(h/\lambda)\eta$ and $\Delta V/V|_{\text{Au}} = -13.9(h/\lambda)\eta$.

These expressions illustrate that mechanical loading for the Al/GaAs and Al/Si systems only slightly influences the SAW velocity and hence the center frequency, in contrast to systems using gold as the grating material. For the present case, the ratio of the bar height to the grating period, $h/p = 0.227$, suggests that a better approximation would be obtained by retaining higher order terms in the velocity correction. However, the results presented in this paper, in addition to previous efforts by Bonello *et al.*,¹¹ confirm that for an aluminum grating on a Si substrate the effect of mechanical loading on the SAW propagation velocity is small.

A quantitative comparison between the generation efficiency for the Si and GaAs samples would require a calibrated detection scheme, however, a qualitative comparison can be made by considering the signal to noise ratios for the two samples. The signal to noise ratio is larger for the Si sample than for the GaAs sample, which is likely due to the larger metallization duty cycle used for the GaAs sample. Another factor contributing to the difference in signal to noise is the ability to generate a substantial thermal gradient in a direction parallel to the SAW propagation vector. This lateral thermal gradient to a large extent is governed by the lateral modulation of the energy density of the absorbed pump light. For a pump wavelength of 395 nm, the optical skin depth for Si and GaAs is 82 and 15 nm, respectively. Thus for an aluminum grating, skin depth ~ 10 nm, it is expected that the Si system will more efficiently generate SAW's at a frequency corresponding to the grating period than the GaAs system. In addition to generation efficiency, it would be natural to address acoustic attenuation. However, given that the emphasis of this experiment involved investigating standing SAW's in the grating region only, no effort was made to distinguish between attenuation due to mechanical loading and other forms of acoustic attenuation.

In summary, we have demonstrated generation and detection of suboptical wavelength picosecond SAW's. Acoustic generation and detection was achieved by using electron beam lithography to modulate the surface absorption characteristics on a suboptical wavelength scale. The generation and detection characteristics of the absorption grating were investigated as a function of optical polarization. For the 790-nm-probe beam, the absorption grating acted as an optical polarizer, however, for the 395-nm-pump beam, the absorption characteristics of the grating were only slightly polarization sensitive. Two material systems were investigated, aluminum gratings on Si and GaAs substrates. The experimentally determined center frequencies were 22 and 13 GHz for the Si and GaAs sample, respectively. These frequencies correspond closely to the frequencies predicted using the SAW velocity of the substrate materials and the grating period, confirming that for both the Al/GaAs and Al/Si sample, the effect of mechanical loading on the propagation velocity is small. Furthermore, the results presented in this paper support the view that utilization of metallic gratings for SAW generation involves thermoelastic⁶ production of guided longitudinal waves that propagate down the thickness of the bars launching SAW's upon reaching the bar/substrate inter-

face. The ability to generate and detect suboptical wavelength picosecond SAW's opens up new avenues of investigation for probing near-surface physical processes at the nanometer scale.

We are grateful to Dr. Oliver Wright of Hokkaido University for valuable discussions regarding various picosecond

acoustic generation modalities and Mathew Delong and Sergey Li of the University of Utah for producing high quality lithographic gratings. This work was sponsored by the U.S. Department of Energy, Office of Science-BES, Materials and Engineering Physics program and the Laboratory Directed Research and Development program under DOE Idaho Operations Office Contract No. DE-AC07-99ID13727.

-
- ¹G. Tas and H. J. Maris, *Phys. Rev. B* **49**, 15 046 (1994).
²V. Gusev and O. B. Wright, *Phys. Rev. B* **57**, 2878 (1998).
³H. Y. Hao and H. J. Maris, *Phys. Rev. Lett.* **84**, 5556 (2000).
⁴D. H. Hurley, O. B. Wright, O. Matsuda, V. E. Gusev, and O. V. Kolosov, *Ultrasonics* **38**, 470 (2000).
⁵C. Thomsen, H. T. Grahn, H. J. Maris, and J. Tauc, *Phys. Rev. B* **34**, 4129 (1986).
⁶V. E. Gusev and A. A. Karabutov, *Laser Optoacoustics* (AIP, New York, 1993), pp. 93–134.
⁷D. H. Hurley and O. B. Wright, *Opt. Lett.* **24**, 1305 (1999).
⁸O. B. Wright, *Phys. Rev. B* **49**, 9985 (1994).
⁹Y. Sugawara, O. B. Wright, O. Matsuda, M. Takigahira, Y. Tanaka, S. Tamura, and V. E. Gusev, *Phys. Rev. Lett.* **88**, 185504 (2002).
¹⁰H. N. Lin, H. J. Maris, L. B. Freund, K. Y. Lee, H. Luhn, and D. P. Kern, *J. Appl. Phys.* **73**, 37 (1993).
¹¹B. Bonello, A. Ajinou, V. Richard, Ph. Djemia, and S. M. Cherif, *J. Acoust. Soc. Am.* **110**, 1943 (2001).
¹²The square of the mass density for gold is 50 times that of aluminum.
¹³B. Stenkamp, M. Abraham, W. Ehrfeld, E. Knappek, M. Hintermaier, M. T. Gale, and R. Morf, *Proc. SPIE* **2213**, 288 (1994).
¹⁴The absorption grating serves to modulate the surface reflectivity on a length scale that is smaller than the optical wavelength of the pump and probe beam. Consequently, the absorption characteristics of the grating are similar to a wire-grid polarizer.
¹⁵G. L. Eesley, *Phys. Rev. B* **33**, 2144 (1986).
¹⁶H. Tamada, T. Doumuki, T. Yamaguchi, and S. Matsumoto, *Opt. Lett.* **22**, 419 (1997).
¹⁷In the present case, the pump spot size is approximately 2 microns and the repeat length is 220 nm, thus the majority of the SAW energy is produced at the mini Brillouin zone boundary π/p .
¹⁸J. Koskela, V. P. Plessky, and M. M. Salomaa, *IEEE Trans. Ultrason. Ferroelectr. Freq. Control* **45**, 439 (1998).
¹⁹B. A. Auld, *Acoustics Fields and Waves in Solids* (Wiley-Interscience, New York, 1973), Vol. 2, pp. 151–162.
²⁰S. Datta and B. J. Hunsinger, *J. Appl. Phys.* **50**, 5661 (1979).
²¹H. Robinson, Y. Hahn, and J. N. Gau, *J. Appl. Phys.* **65**, 4573 (1989).